Surface Modification of Aramid Fibers with γ-Ray Radiation for Improving Interfacial Bonding Strength with Epoxy Resin

Yanhua Zhang, Yudong Huang, Li Liu, Lina Wu

Department of Applied Chemistry, Harbin Institute of Technology, Harbin 150001, People's Republic of China

Received 13 January 2007; accepted 1 May 2007
DOI 10.1002/app.26887
Published online 25 July 2007 in Wiley InterScience (www.interscience.wiley.com).

ABSTRACT: Co^{60} γ-ray radiation as a simple and convenient method for surface modification of Armos aramid fibers was introduced in this article. Two kinds of gas mediums, N_2 and air, were chosen to modify aramid fiber surface by γ-ray irradiation. After fiber surface treatment, the interlaminar shear strength values of aramid/epoxy composites were enhanced by about 17.7 and 15.8%, respectively. Surface elements of aramid fibers were determined by XPS, the analysis of which showed that the ratio of oxygen/carbon was increased. The crystalline state of aramid fibers was determined by X-ray diffraction instrument. The surface topography of fibers was analyzed by atomic force microscopy and scanning electron microscope. The degree of surface roughness and the wettability of fiber surface were both enhanced by γ-ray radiation. The results indicated that γ-ray irradiation technique, which is a suitable way of batch process for industrialization, can significantly improve the surface properties of aramid fibers reinforced epoxy resin matrix composites. © 2007 Wiley Periodicals, Inc. J Appl Polym Sci 106: 2251–2262, 2007

Key words: aramid fibers; surface treatment; γ-ray irradiation; interfacial properties

INTRODUCTION

Aramid fibers, owing to its low density, high tenacity, and high modulus, are a good candidate as the reinforcement for polymer composites in aircraft, aerospace, and missile application. At present, Armos fibers are the most excellent aramid fibers in commercial process on a large scale. Less regular molecular chain structure of Armos fibers leads to a higher number of stress-holding (stress-withstanding) molecular chains, and therefore, Armos fibers hold a maximum number of mechanical properties in comparison to all other aramid fibers.[1] However, the surface of Armos fibers is so chemically inert and smooth that the adhesion, between fibers and the resin matrix, is poor. Hence, surface modification is essential for aramid fibers to enhance the interfacial adhesion strength. Various approaches of surface modification for aramid fibers have been developed, such as chemical, physical treatments, and the coalescence of the two methods.

The chemical method includes all kinds of acid solutions treatment,[2–4] bromoacetic acid and chlorohydrin treatment,[5] acetic anhydride treatment,[6] acrylamide grafting,[7] and rare earth modifier grafting modification of aramid fibers' surface treatment.[8] The physical method is mainly ultrasound treatment.[9] The third method mainly contains plasma treatment and polymerization.[10–13]

Most of the aforementioned experimentation methods are only carried out in laboratories. Radiation processing was used earlier for polymer modification. The irradiation of polymeric materials with ionizing radiation (γ-rays, X-rays, accelerated electrons, ion-beams) leads to the formation of very reactive intermediates, free radicals, ions, and excited states. These intermediates can follow several reaction paths that result in disproportion, hydrogen abstraction, arrangements, and/or the formation of new bonds. Since γ-rays have so strongly penetrating power, γ-ray irradiation is therefore particularly applicable to bulky products and even single pieces measuring a few m^3 are routinely irradiated.[14] The γ-ray irradiation treatment method of fiber surface modification has several advantages over other treatments. The primary one is that the mechanical properties of the fibers are not reduced in substance if the conditions are controlled. Another advantage is clean, saving energy and more efficient treatment. Currently, γ-ray irradiation was widely applied to the polymer materials in the last 5 years, such as the preparation of polymers, the graft-

Correspondence to: Y. Huang (huangyd@hit.edu.cn).
Contract grant sponsor: National Natural Science Foundation of China; contract grant number: 50333030.
Contract grant sponsor: Natural Science Foundation of Heilongjiang for Distinguished Young Scholars; contract grant number: JC04-12.

ing on polymers and the effect of polymers by γ-ray irradiation technology and so on. The polymers, synthesized by γ-ray irradiation polymerization technique contain the biopolymer hydrogels,[15] ''gradient'' polymer (in which the instantaneous composition varies continuously along the chain contour),[16] acrylic rubber,[17] semi-interpenetrating polymer networks of poly(3-hydroxybutyrate),[18] diethyl fumarate,[19] methyl acrylate,[20] and poly(*N*-vinyl-2-pyrrolidone–crotonic acid) copolymers[21] were synthesized by γ-ray irradiation polymerization technique. The polymers grafted by γ-ray irradiation include the high-density polyethylene films,[22] ultra-high-modulus fibers,[23] polypropylene,[24] and polyethylene terephthalate.[25] The polymers explored were affected by γ-ray irradiation technology, which contain PolyNIMMO [poly (3-nitratomethyl-3-methyloxetane)],[26] polyurethane.[27] Of course, films and fibers are included in these polymers. The films are poly (ethylene-*co*-tetrafluoroethylene) film,[28] polyethylene film,[29] polyethylene terephthalate film,[30] films of piezoelectric PVDF and P(VDF-TrFE).[31] The fibers are high-strength ultrahigh-molecular-weight polyethylene,[32] ramie,[33] carbon,[34] and PBO.[35] Consequently, γ-ray radiation seems to be an alternative technique for surface treatment of aramid fibers.

In this article, aramid fibers were treated in N_2 and air medium by γ-ray radiation. The effect of the different irradiation doses on the aramid fiber surface and the interfacial properties of aramid fibers/epoxy resin composites were investigated. The surface characteristics of aramid fibers were evaluated by X-ray photoelectron spectroscopy (XPS), scanning electron microscope (SEM), and atomic force microscopy (AFM). The crystalline state of fibers was determined by X-ray diffraction (XRD) instrument. The fiber surface free energy was also measured. The single fiber tensile test was carried out to study the influence of γ-ray radiation on fiber mechanical strength. The interfacial properties of composites were employed by ILSS testing.

EXPERIMENTAL DETAILS

Materials

The aramid fibers used were Armos fibers (average diameter 16.7 μm, density 1.43 g/cm^3, tenacity 4.5–5.5 GPa, elasticity modulus 140–160 GPa), which were obtained from ''Tverchimovolokno'' J.-S., Russia. Epoxy resin (E-51) was supplied by Wuxi Resin (Wuxi, China). Tetrahydrophthalic anhydride (THPA) was used as curing agent and benzyldimethylamine as curing accelerating agent.

γ-Ray irradiation treatment

Cobalt-60 was selected as the radiation source in this research. The irradiation field was provided by Harbin Rui Pu Irradiation New Technology Company, China. Armos fibers were dried at 100°C for 3 h in a vacuum drying oven before being used. Fiber bundles were entwined on the frame and then put into the glass container. Two kinds of gas mediums, air and N_2, were chosen. In air medium, air was directly sealed in the container. In N_2 medium, the container was vacuumized by means of a vacuum pump at one end of it and then N_2 was pressed into it at the other end. In succession it was tightly sealed. The sketch map is shown in Figure 1. Finally, the samples were placed into the Co point-source radiator and irradiated by different absorption doses.

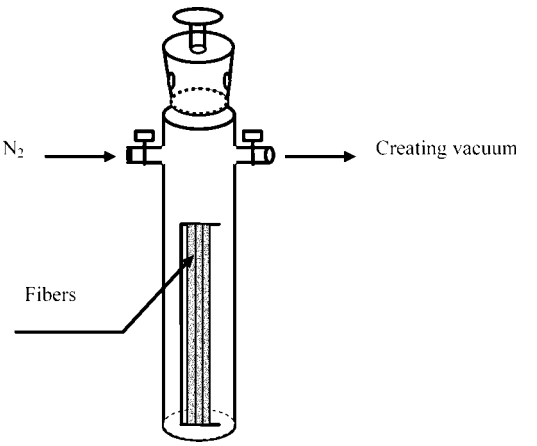

Figure 1 Schematic of the irradiation instrument.

Preparation of the aramid fibers/epoxy resin composites

The unidirectional, long Armos fibers reinforced epoxy composites were made with both untreated and radiation-treated fibers. These unidirectional composite specimens were fabricated by combining fibers with epoxy resin E-51 through a compression molding processing method. The curing system was made of epoxy resin E-51, THPA as curing agent, and benzyldimethylamine as the accelerating agent, which was mixed at the ratio of 100 : 70 : 1 by mass, respectively. The content of the resin in composites was controlled at about 38 mass %. The curing process used is as follows: 90°C for 2 h, 120°C for 2 h, and 150°C for 4 h. During the curing process, the 3 MPa pressure value was loaded after the temperature being increased to 90°C, and kept for 20 min, because the resin shows long continuous filament by tension at that time. When the temperature increased to 120°C, the 10 MPa pressure value was loaded. The mold was cooled to room temperature with the pressure being maintained, and thus the curing process was completed. All composite samples were about 6.5 mm in width and 2 mm in thickness.

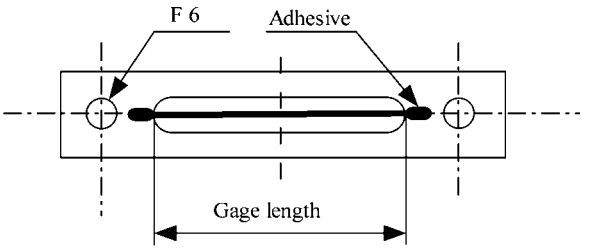

Figure 2 Schematic of the single fiber tensile specimen.

Single fiber tensile test of aramid fibers

The single fiber quasistatic tensile test was conducted following the recommended testing procedures as in ASTM C 1557-03/JIS R 7601. The sketch map in Figure 2 illustrates the single fiber tensile test specimen. The single fiber was glued to the paper sample frame. The gage length is 25 mm and the test was carried out at room temperature. Each data entry was the average of at least 50 or more samples. The tensile strength of the single fiber was calculated as following:

$$\sigma_t = \frac{4F_b}{\pi d^2} \quad (1)$$

where σ_t = tensile strength in Pa, F_b = to force to failure in newton, and d = fiber diameter in meters.

Interfacial characterization of aramid fibers/epoxy resin composites

The interlaminar shear strength (ILSS) of aramid/epoxy composites were tested on an universal testing machine (WD-1, Changchun, China) using a three-point short-beam shear test method according to ASTM D 2344-76. The sketch map is shown in Figure 3. Specimen dimensions were 20 mm × 6 mm × 2 mm, with the span to thickness ratio of 5. The condition of the specimen and an enclosed space where test was conducted were maintained at room temperature. The specimens were tested at the rate of cross-head speed 2 mm/min. ILSS, Γ, for the short-beam test was calculated according to the following expression:

$$\Gamma = \frac{3P_b}{4bh} \quad (2)$$

where P_b is the maximum compression load at fracture in newton, b is the width of the specimen in mm, and h is the thickness of the specimen in mm. Each reported ILSS value was the average of more than eight successful measurements.

XRD test of aramid fibers

The crystalline state of aramid fibers, including the untreated and the γ-radiation-treated, was determined using XRD instrument.[36] The apparatus is DMAX-12 kW rotating anode XRD instrument from Japan. The adequate length Armos fibers were homogeneously laid on the aluminum plate, which has a circular cavity, and then the two ends of fibers were fixed on the aluminum frame with the double-faced adhesive tape. The specimens were used for XRD test. The test condition was as following: Cu Kα-radiation, graphite crystal as the monochromator, wavelength λ = 1.5418 × 10^{-10} m, tube voltage 40 kV, current 40 mA, sequential scanning counting mode. The standards employed were DS 1°, SS 1°, and RS 0.15 mm.

Surface element analysis of aramid fibers

It is well known that XPS is a very useful technique in the determination of chemical composition and functional groups of the fiber surface, and the testing depth is about 5 nm. The surface composition, as measured by XPS, can be understood easily and related to the fibers. Both the untreated aramid fibers and those subjected to γ-ray irradiation treatment were successfully Soxhlett extracted with acetone solvent after 72 h and then dried in vacuum drying oven. The specimens were cut into a certain length and affixed on a sheet metal for testing. XPS was used to analyze changes in the proportions of elements such as C, N, and O and their chemical valence on the surface of aramid fibers according to GB/T 19500-2004. XPS analysis was performed by Thermo ESCALAB 250 (Thermo VG Scientific, UK) equipped with Mg Kα (1253.6 eV) Mono X-Ray Source. The test conditions were a pressure range of 10^{-8} to 10^{-9} Torr, power of 150 W, and electric pressure of 15 kV.

Observations of fiber surface morphology by SEM and AFM

SEM is usually used to observe fiber surface and fiber fracture topographies. Here, both the topogra-

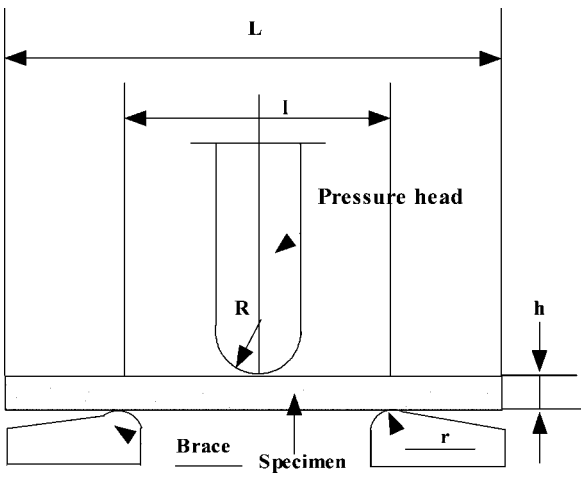

Figure 3 Schematic of ILSS testing device.

phies of fiber surface and the tensile fracture of single fiber were investigated. Due to the poor conductivity of aramid fibers, the samples were fixed on the aluminum plate via a conducting adhesive and then degassed sputter coated with gold for 4–5 min to provide a conducting path for the impinging electrons. Thus a thin layer of gold, 10 nm in thickness, was coated at the surface of the fibers. Individual fiber was examined in the S 4700 SEM (Hitachi, Japan) which employs a field emission gun. Typical values of voltage and working distance of operation were 20 kV and 7–10 mm, respectively. SEM was successfully employed for obtaining morphological details of the fiber up to micronscale resolution.

The surface morphological details at submicron resolution were observed by AFM in the no-contact mode. A multimode AFM Solver P47 (NT-MDT, Moscow, Russia) was used to investigate the topography of the fiber surface. A single Armos fiber is fastened to a steel sample mount using the tapping mode. Roughness analysis is carried out from the images obtained over a 4 μm × 4 μm area.

Surface free energy measurement of aramid fibers

Aramid fiber surface energy (γ_f^T) and its dispersive component (γ_f^d) and polar component (γ_f^p) were determined by dynamic contact angle analysis (DCAA) on the wettability testing device (SB213; Keen, Beijing, China). All the measurements were carried out with a dynamic capillary method. In the experiment, a bundle of fibers was aligned and inserted into a polyethylene tube with diameter 2 mm and length 50 mm. Then 1 mm length of fibers sample was left outside the tube. The fiber bundle sample was suspended on the hook of a precision balance. The end of the bundle was impregnated in the liquid. As soon as the end of the bundle began to impregnate the liquid, the wetting mass and time were both recorded by computer. The testing process went on until the point of wetting equilibrium, i.e., until the liquid was no longer adsorbed by the fiber bundle. The second vaporized water and the normal octane were chosen. Then the contact angle between wetting liquid and aramid fibers can be calculated according to eqs. (3) and (4):

$$\Delta\gamma = \frac{0.064H^2\ \rho_f\ \eta}{d_f K^2 W_f \rho^2} \frac{(1-\varepsilon)^2}{\varepsilon^3} \frac{1}{V_T} \frac{m^2}{t} \tag{3}$$

$$\cos\theta = \frac{\Delta\gamma}{\gamma_l} \tag{4}$$

where $\Delta\gamma$ is the surface free energy of the difference between dry and wet unit surface; H is the height of fiber bundle; ρ_f is the density of Armos fibers; η is the viscosity of the wetting liquid; ε is the void volume fraction in the tube (between 0.48 and 0.52); m is the mass of the wetting liquid adsorbed by the fibers at immersion equilibrium; d_f is the diameter of the fiber; K is the hydraulic constant; W_f is the weight of the fiber bundle before immersion; ρ is the density of the wetting liquid; V_T is the total volume of the body system; t is the time of the immersion equilibrium; θ is the dynamic contact angle between the fibers and the immersion liquid; γ_l is the surface tension of the wetting liquid. The dynamic contact angle is used to calculate the fiber surface free energy according to Kealble equation.[37]

TABLE I
Surface Free Energy of the Liquids at Room Temperature

	Surface tension (dyn/cm)		
	γ_l^T	γ_l^d	γ_l^p
Second vaporized water	72.8	21.8	51.0
Normal octane	21.8	21.8	0

$$\gamma_l^T(1+\cos\theta) = 2\left(\gamma_l^p\gamma_f^p\right)^{1/2} + 2\left(\gamma_l^d\gamma_f^d\right)^{1/2} \tag{5}$$

$$\gamma_f^T = \gamma_f^d + \gamma_f^p \tag{6}$$

γ_f^T, γ_f^d, and γ_f^p are the total surface free energy, dispersive component energy, and polar component energy of the fibers, respectively; γ_l^T, γ_l^d, and γ_l^p are the surface tension of an immersion liquid and its dispersive and polar component, respectively. The surface free energy values of the liquids used in experiments are listed in Table I.[38] The value of test is more than 20 successful measurements.

RESULTS AND DISCUSSION

Interfacial properties of aramid/epoxy composites

The effect of γ-ray radiation treatment on the composites' interfacial adhesion property was carried out using ILSS test of aramid/epoxy composites. Figures 4 and 5 accordingly show the effect of irradiation doses, in air and N_2 medium, on the ILSS of the aramid/epoxy composites system. All the ILSS of the composites, whose fibers were treated by γ-ray radiation, were improved to some extent. The effect tendency of irradiation doses on the ILSS was similar in two kinds of medium. That is, to say in detail, the increasing ILSS value was rising at first and then running down as shown in Figures 4 and 5. This suggests that γ-ray radiation is a very efficient treatment method in improving fibers–matrix adhesion. The value of ILSS reached the maximum at 600 kGy. Namely, the values of ILSS are 71.3 MPa in N_2 and

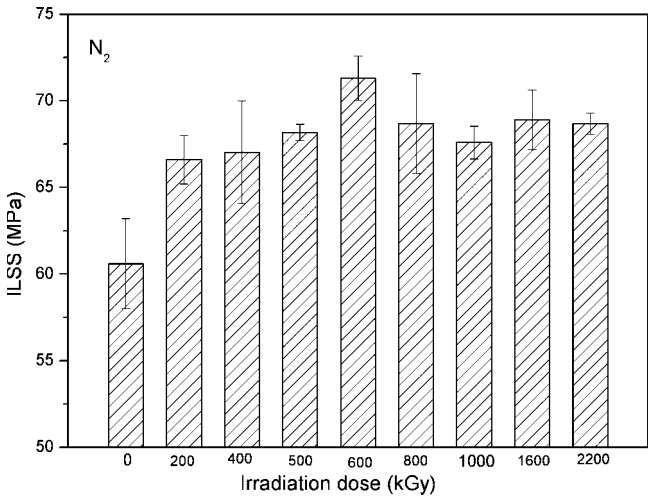

Figure 4 ILSS of Armos/epoxy composites untreated and treated with different irradiation doses in N_2.

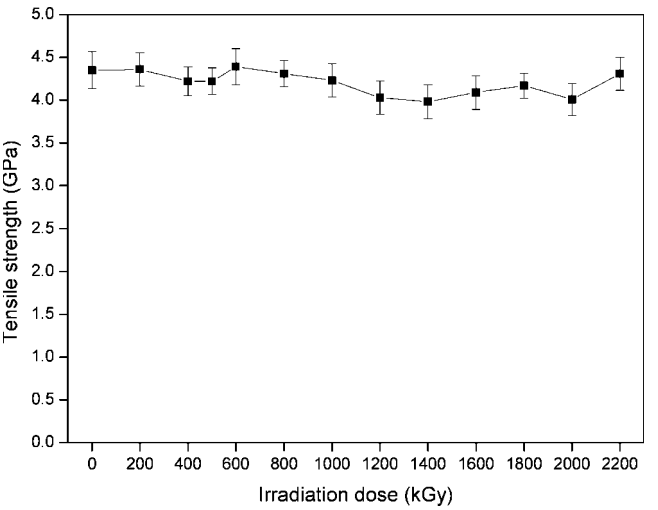

Figure 6 Single tensile strength of Armos fiber in air with different irradiation doses.

70.1 MPa in air. There are 17.7 and 15.8% improvement compared with the untreated sample whose ILSS value was 60.59 MPa, respectively. So the most optimal irradiation doses in the two medium were also 600 kGy. The results show that a better fiber/matrix interface adhesion was obtained at 600 kGy irradiation dose.

Remark: 0 kGy is referred to the untreated fibers in this article.

Single fiber tensile strength of aramid fibers and Weibull analysis

The change of single fiber tensile strength in air with the increasing irradiation dose was recorded as shown in Figure 6. The untreated aramid fiber had the tensile strength of 4.35 GPa. It showed that the strength of 600 kGy treatment was 4.39 GPa greater than the strength of other irradiation doses which were less than that of the untreated fiber. A minor reduction in tensile strength is only subter-3% at the irradiation dose range of less than or equal to 1000 kGy. In fact the decreasing value can be neglected because it is wholly within the range of experiment error. Whereas, in the irradiation dose range from 1200 to 2200 kGy, the tensile strength can be kept up more than 4 GPa. The single fiber tensile strength in N_2 with γ-ray radiation is similar to that in air at the same irradiation dose. It is obvious that surface modification method of aramid fibers with γ-ray radiation does not badly impair the tensile property of aramid fibers in substance, or the damage degree of the method is very low. It is the optimal result anticipated. This offers the best supporting to surface modification of aramid fibers with γ-ray radiation.

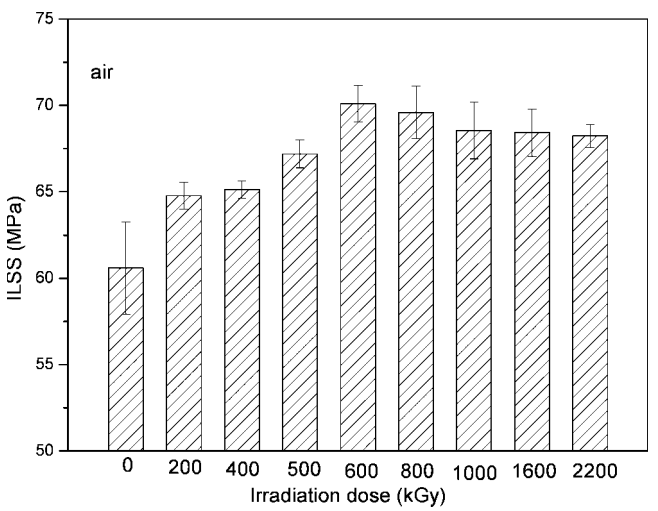

Figure 5 ILSS of Armos/epoxy composites untreated and treated with different irradiation doses in air.

The tensile strength of the single fiber is generally analyzed by the well-known Weibull statistics, and so the strength of the fiber obeys the two parameters expressed by the empirical equation:

$$F(\sigma_f) = 1 - \exp\left[-L(\sigma_f/\sigma_0)^{\beta}\right] \quad (7)$$

where σ_f is tensile strength, $F(\sigma_f)$ is the failure probability of an individual fiber at an applied stress of σ_f, L is the ratio of length about the reference length, σ_0 is the scale parameter, β is the shape or flaw dispersion parameter. Equation (7) can be rearranged as:

$$\ln\ln\left[1/\left(1 - F(\sigma_f)\right)\right] = \beta \ln\sigma_f + \ln L - \ln\sigma_0^{\beta} \quad (8)$$

A linear regression analysis can be applied to a plot of ln ln $[1/(1 - F(\sigma_f))]$ vs. ln σ_f. So σ_0 and β are obtained by the slope and intercept of this line. The Weibull probability plots for tensile strength of the untreated and 600 kGy are shown in Figures 7 and 8.

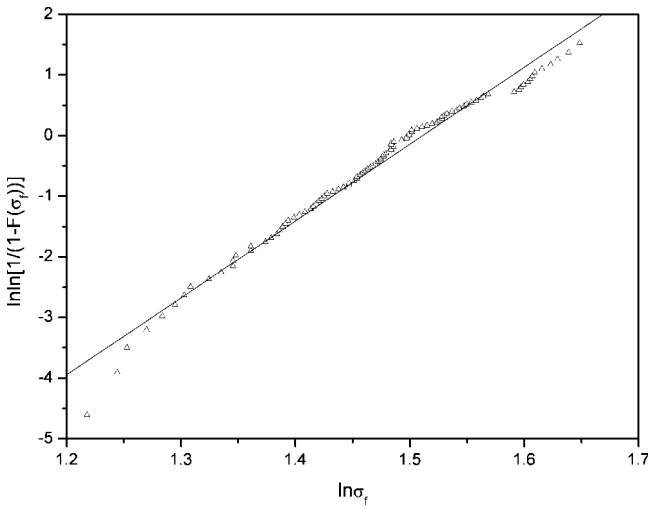

Figure 7 Weibull plots of the untreated Armos fiber strength.

Values of Weibull parameters obtained from linear regression analysis of fibers with different irradiation doses are given Table II.

The experimental data can be ranked in ascending order of strength values and the cumulative probability $F(\sigma_f)$ can be assigned as

$$F(\sigma_f) = n/(N+1) \tag{9}$$

where n is the rank of the tested fiber in the ranked strength tabulation and N is the total number of fibers tested.

XRD analysis

Irradiation doses (0–1000 kGy) were chosen in N_2 to be analyzed by XRD instrument according to the results from the Interfacial Properties of Aramid/Epoxy Composites section. Figure 9 is XRD spectra of Armos fibers in N_2. There is no distinct variety from XRD spectra which illuminated radiation did not change the crystal type. Figure 10 shows the change in the diffraction angle 2θ with different irradiation doses. 2θ with the increasing the irradiation doses ascended step by step, rapidly arriving at the maximum (600 kGy), and then promptly descended. It illustrated that the crystallinity of Armos fibers after γ-ray irradiation maybe varied slightly. Figure 11 illustrated that the change of the irradiation doses influenced on the interplanar distance. It is obviously seen that the interplanar distance reached the minimum value at 600 kGy. γ-ray is a sort of electromagnetic wave, which holds strongly penetrating power, and it acts on the Armos fibers (a kind of crystalline polymers) mainly through the Compton effect. Firstly, the breakage happened near the N and O groups so that the free radicals of high activity come into being. Then these free radicals renew-

TABLE II
Weibull Parameters for Tensile Strength of Fibers

Armos fibers	Slope	Intercept	β	σ_0	σ_f (GPa)
Untreated	12.68	−19.16	12.68	3.33	4.35
200 kGy	13.90	−21.00	13.9	3.42	4.36
400 kGy	12.17	−18.02	12.17	3.19	4.22
500 kGy	11.55	−17.13	11.55	3.14	4.22
600 kGy	12.46	−18.93	12.46	3.34	4.39
800 kGy	11.03	−16.61	11.03	3.16	4.31
1000 kGy	12.43	−18.59	12.43	3.25	4.23
1200 kGy	12.83	−18.38	12.83	3.09	4.03
1400 kGy	12.92	−18.33	12.92	3.05	3.98
1600 kGy	10.81	−15.73	10.81	2.98	4.09
1800 kGy	12.21	−17.94	12.21	3.15	4.17
2000 kGy	11.41	−16.32	11.41	2.97	4.01
2200 kGy	9.33	−14.12	9.33	2.99	4.31

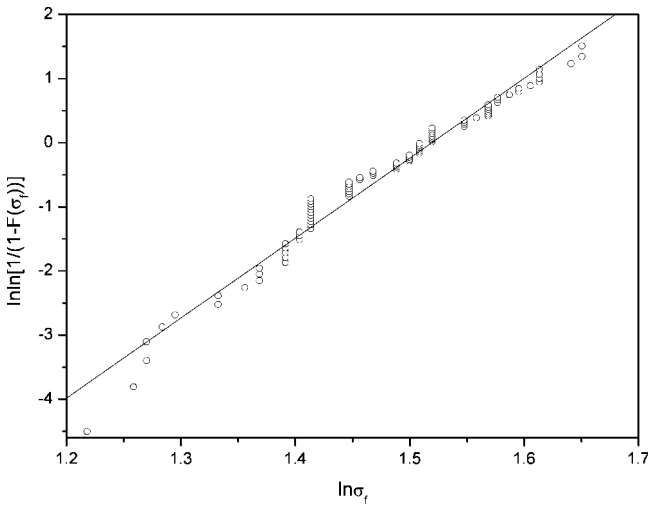

Figure 8 Weibull plots of the Armos fiber strength treated with 600 kGy γ-ray radiation.

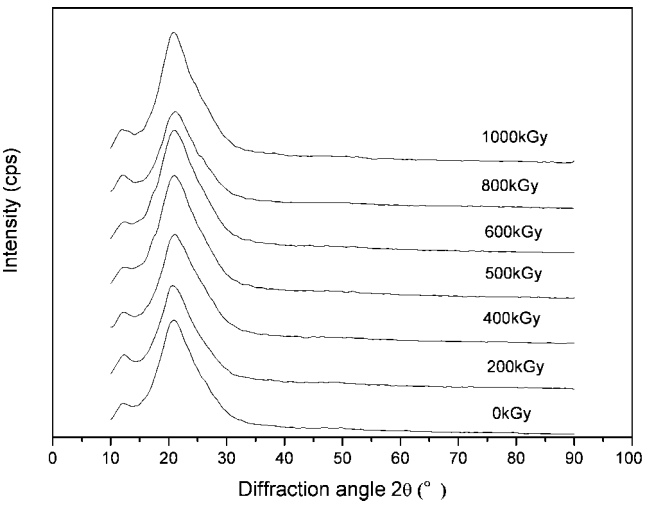

Figure 9 XRD spectra in N_2 with different irradiation doses.

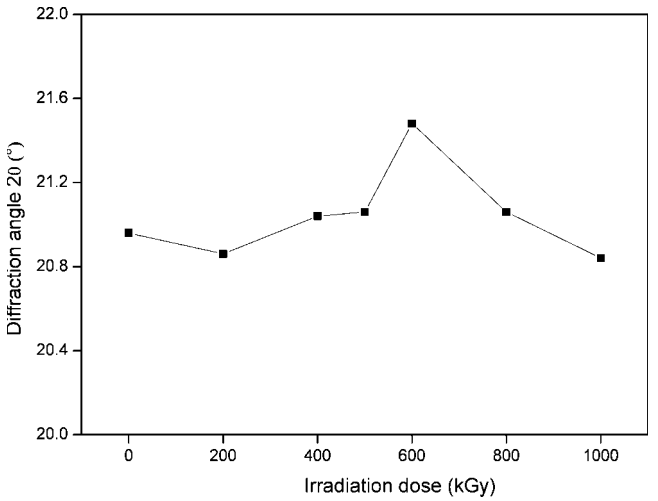

Figure 10 The effect of irradiation doses on diffraction angle 2θ.

edly assembled and further formed the cross bonds. Thus the regional reticular structure gradually came into being with the increase of the cross bonds up to the formation of the integral network configuration. So the crystallinity of Armos fibers can be changed after γ-ray radiation by right of the aforementioned mode. Certainly the diffraction angle 2θ and the interplanar distance correspondingly changed. These offered theoretic proof for that aramid/epoxy composite achieved the best adhesion property at 600 kGy γ-ray radiation.

XPS analysis

The survey spectra were obtained to identify the fiber surface elements present and to carry out a quasiquantitative analysis. The surface composition

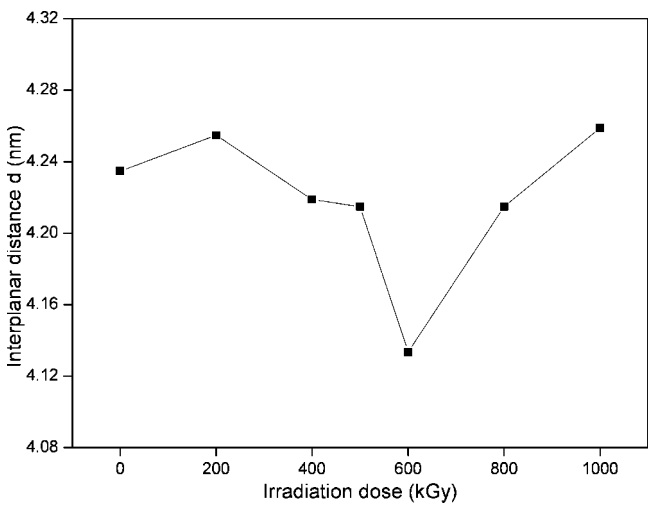

Figure 11 The effect of irradiation doses on the interplanar distance *d*.

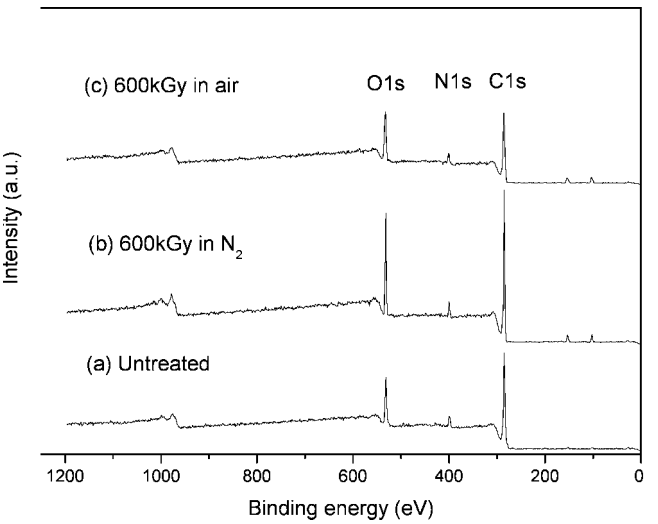

Figure 12 X-ray photoelectron spectra of (a) untreated Armos fibers, (b) 600 kGy γ-ray radiation in N_2, and (c) 600 kGy γ-ray radiation in air.

of the Armos fibers was analyzed by XPS, and the result of wide-scan spectra was shown in Figure 12, where (a) is the spectrum of the virgin fibers, (b) refers to the fibers with 600 kGy γ-ray radiation in N_2, and (c) is 600 kGy in air. The XPS survey spectra showed distinct carbon, oxygen, and nitrogen peaks, which represented the major element constituents of the Armos fibers. A small quantity of chlorine was also observed from the spectrum. This chlorine had been assigned to as coming from the Cl-containing residues perhaps due to the monomer remained when the fibers matrix was synthesized. Changes in elements on the surface of Armos fibers are given in Table III. The N1s/C1s ratio and O1s/C1s ratio of the virgin fibers are 0.068 and 0.206, respectively. While after γ-ray radiation, the values were 0.053 and 0.254 in N_2, then correspondingly 0.074 and 0.258 in air. The ratio of O1s/C1s of fibers treated was enhanced, which indicated the polar groups on fibers surface were increased. It is well known that the surface oxygen content has been reported to be crucial for good wetting and bonding of resin.[6,7,39] The fibers with γ-ray radiation treatment offered so better wetting and bonding of resin that the mechanical interfacial properties between fiber and the matrix were remarkably improved.

TABLE III
Surface Element Composition Analysis of Armos Fibers Untreated and After Irradiation Treated

Armos fibers	C1s (%)	O1s (%)	N1s (%)	Cl2p (%)	O/C	N/C
Untreated	78.11	16.07	5.28	0.53	0.206	0.068
600 kGy + N_2	76.36	19.4	4.04	0.19	0.254	0.053
600 kGy + air	74.81	19.27	5.53	0.38	0.258	0.074

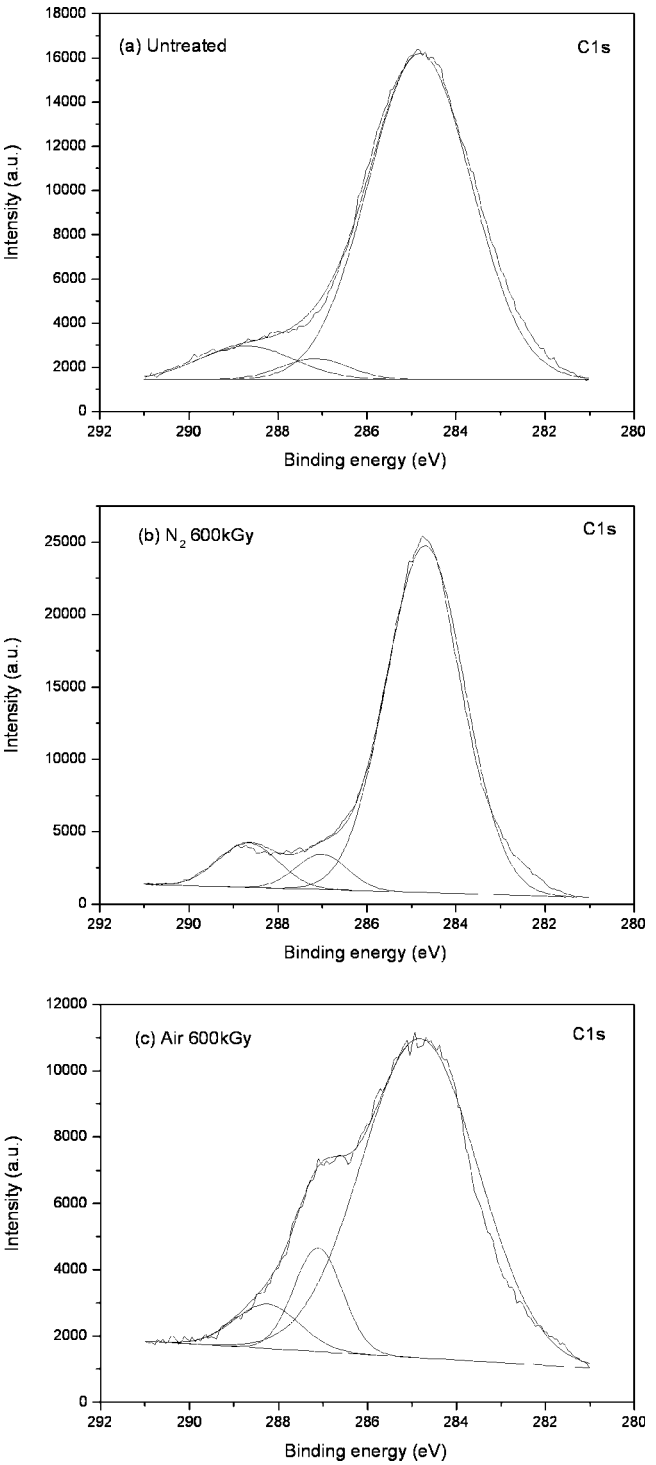

Figure 13 Deconvolution of the C1s peak spectrum by XPS analysis of Armos fibers (a) untreated, (b) 600 kGy γ-ray radiation in N_2, and (c) 600 kGy γ-ray radiation in air.

Typical XPS spectra of the C1s peak region at about 285 eV deconvoluted into surface functional group contributions were shown in Figure 13(a–c) for fiber which were untreated, 600 kGy in N_2, and 600 kGy in air treated γ-ray radiation, respectively. Values of the binding energy (BE) and the percent contribution of each curve fit photopeaks were estimated from these curve fit C1s photopeaks listed in Table IV. It was found that the C1s peaks could be fitted to three line shapes. These different BE peaks according to from low to high were assigned as to —C—C— bond (about 284.75 eV), —C—O—, —C—N, —C—Cl, and —C=N bond (about 287 eV), —COO and —CON (about 288.5 eV). The contents of the polar groups were all increased after irradiation treatment, but the degree of rising was different. Therefore, the increasing of the number of oxygen polar groups on the aramid fiber surface plays an important role in improving the adhesion strength between the fibers and epoxy matrix.

The analysis of fiber surface and tensile fracture topography

The surface morphology and the tensile fracture topography of single fiber were analyzed with the aid of SEM. Of course the fibers were made of untreated and after γ-ray radiation in two gas mediums (N_2 and air). Figure 14(a–c) shows SEM photographs for tensile fracture of Armos single fiber. Figure 14(a), which is untreated Armos fiber, showed that fibers fracture feature by tensile splitting and fibrillation of the skin core was commonly observed. It is clear that there is a delaminating cracking of core-skin structure. Figure 14(b,c), which is fibers treated with 600 kGy γ-ray radiation in N_2 and in air, displayed that fiber breakage dispersed homogeneously. The core-skin structure was not distinctly observed. γ-ray radiation ameliorated the core-skin structure of fibers so that the bind strength of the core and skin was intensified. Thus fibers will averagely bear stretching stress.

The surface morphologies of single fiber were shown in Figure 15(a–c). As was seen in Figure 15(a), the surface of untreated fibers was rather smooth, which means that the interfacial adhesion between the untreated fibers and the epoxy resin is poor. However, the surface of the treated fibers in N_2 and

TABLE IV
Contents of Functional Groups on Armos Fibers Before and After Irradiation Treatment

		C1s photopeak		
Armos fibers	Peak assignment	—C—C—	—C—N, —C—O—, —C=N, —C—Cl	—C=O, —CON
Untreated	BE (eV)	284.79	287.15	288.69
	PC (%)	88.1	3.7	8.2
600 kGy + N_2	BE (eV)	284.67	286.99	288.64
	PC (%)	85.9	5.7	8.3
600 kGy + air	BE (eV)	284.8	287.09	288.24
	PC (%)	82.4	11.2	6.4

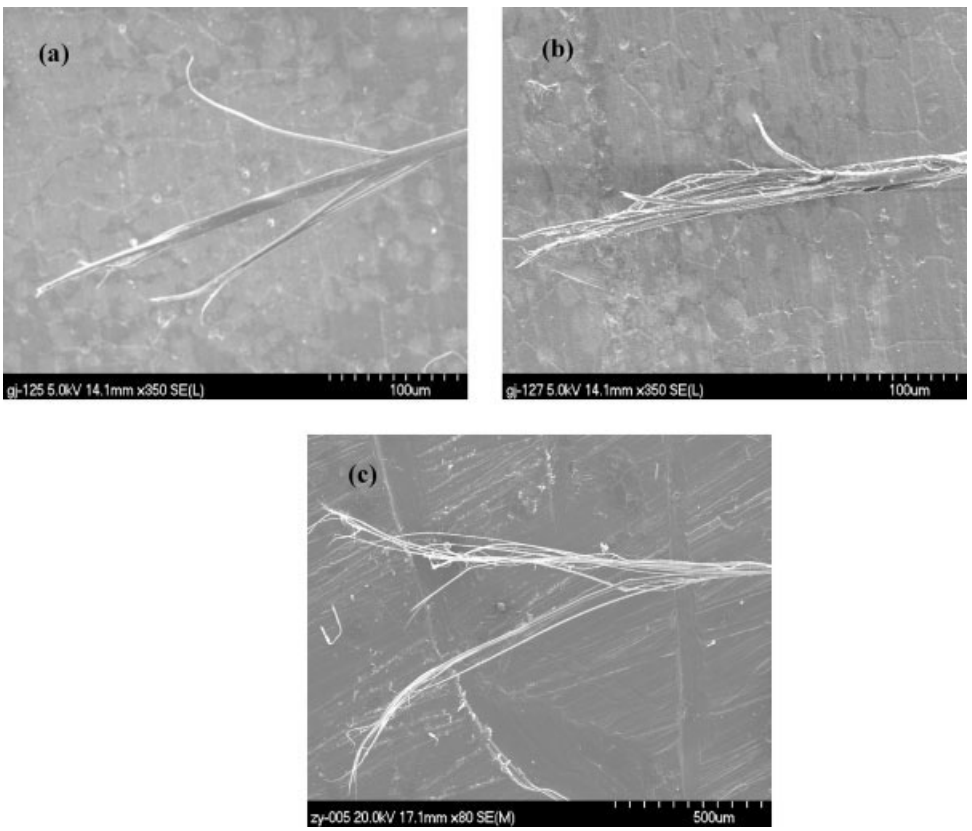

Figure 14 SEM photographs for tensile fractured Armos fiber (a) untreated, (b) 600 kGy γ-ray radiation in N_2, and (c) 600 kGy γ-ray radiation in air.

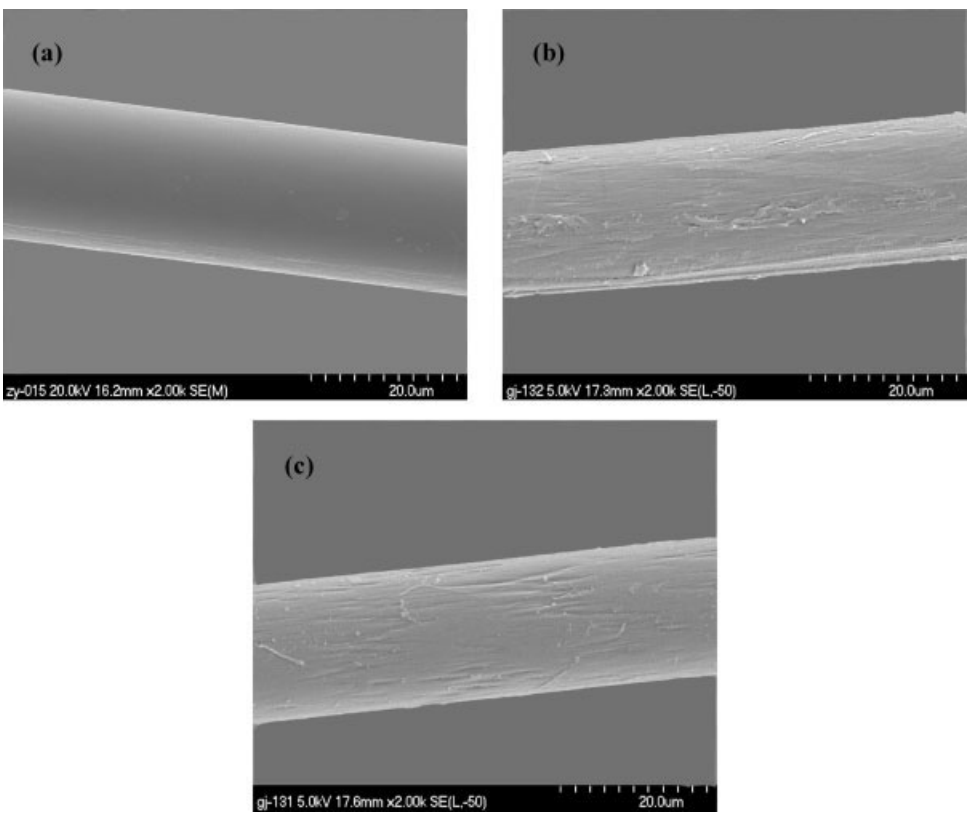

Figure 15 SEM photographs for Armos fiber surface (a) untreated, (b) 600 kGy γ-ray radiation in N_2, and (c) 600 kGy γ-ray radiation in air.

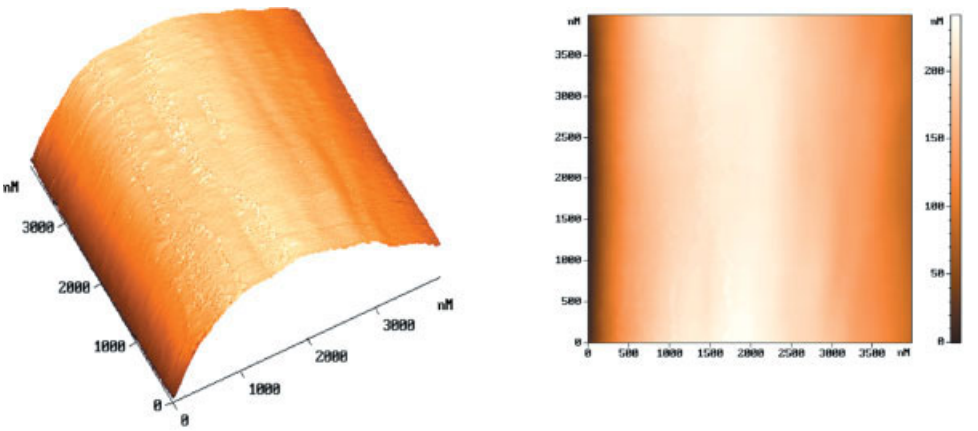

(a) Untreated

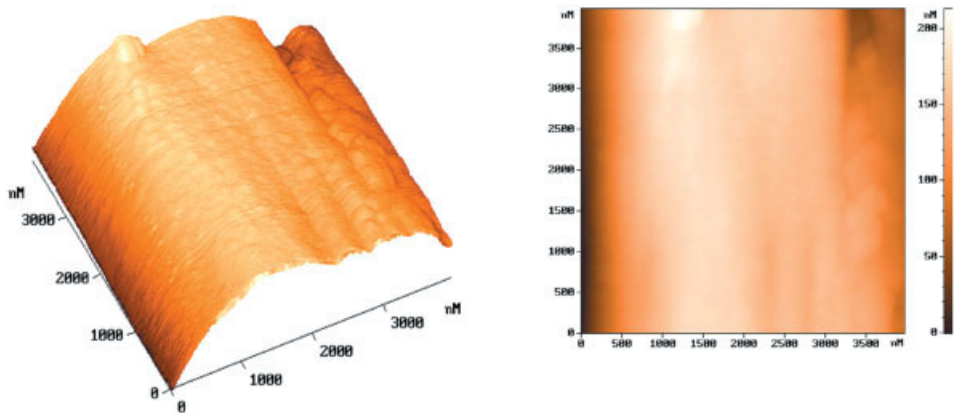

(b) 600 kGy irradiated in N_2

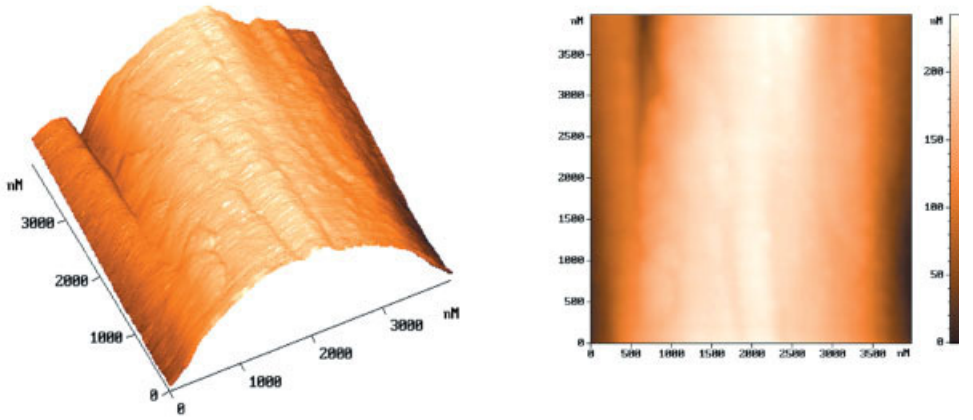

(c) 600 kGy irradiated in air

Figure 16 Three-dimensional and two-dimensional topographies of Armos fibers by AFM. [Color figure can be viewed in the online issue, which is available at www.interscience.wiley.com.]

in air, as shown in Figure 15(b,c), respectively, was much highly rougher in comparison with that of untreated fibers, which is attributed to γ-ray radiation treatment. As seen there were many mild grooves, salient points, and stripes along the fibers axial direction on the surface of the treated fibers. It is well known that the adhesion of the treated fibers to other materials was improved with the increase in the roughness of its surface due to the augment of surface area for bonding and mechanical interlock-

ing. So the rougher surface on Armos fibers is beneficial to improve the adhesion between fiber and matrix, and hence improve the mechanical performance of composites.

AFM was employed to further observe the microscopic morphologies of fiber surface and roughness. Figure 16(a–c) shows the three-dimensional and two-dimensional topography AFM images of untreated, 600 kGy irradiated Armos fibers in N_2 and in air, respectively. In this analysis, the noncontact mode was used. The values of the fiber surface roughness were calculated from two-dimensional topography images using the AFM software. Table V summarized the results of roughness analysis of the irradiated and untreated fibers as obtained from the AFM images. The comparison of the three-dimensional topography AFM images of the fibers showed that irradiation could change the surface topography on a microscopic scale. The surface of the untreated fibers as shown in Figure 16(a) is smooth and few shallow grooves that parallel distributed along with the longitudinal direction of the fibers, because of the characteristic surface structure of Armos fibers. The mean value of peaks height (MVPH) and surface roughness (SR) were 43.3 and 52.3 nm, respectively. From Figure 16(b,c), we could find that the surface topography was changed dramatically after 600 kGy irradiation, the quantity of grooves was increased, and the depth was increased, which were proved by the variation in MVPH (72.6 nm in N_2, 52.0 nm in air) and SR (84.8 nm in N_2, 61.6 nm in air). It could be interpreted by photons etching process on aramid fiber surface. At the same time the fiber surface treated presented large bulge and the roughness of fibers irradiated in N_2 was larger than that in air. This increase in surface roughness should be beneficial for their application as reinforced body in the composite materials, since rougher fiber topography would provide more contact points and lead to a higher degree of mechanical interlocking between the irradiated fiber and matrix. This result provided a strong supporting for increasing the interfacial adhesion between the irradiated fiber and matrix by γ-ray radiation modification of fiber surface.

Fiber surface free energy

The contact angle of the untreated and 600 kGy irradiated in N_2 and air were measured. The results for the two liquids (second vaporized water and normal octane) were determined by DCAAs of aramid fibers. The results obtained for the dispersive and polar components of the surface energy are shown in Table VI. It can be found that the total surface free energy and the polar component of the fibers were increased at 600 kGy, compared with the untreated fibers. The total surface energy of Armos fibers after 600 kGy in N_2 was increased by 24% and in air was enhanced by 23%. The dispersive component of the surface energy after irradiation treatment was raised due to the improvement of fiber surface roughness. The dispersive component of the surface energy of fibers irradiated in N_2 was higher than that in air, which is consistent with the roughness of fibers irradiated in N_2 was larger than that in air. The polar component after 600 kGy irradiation in N_2 was increased from 12.9 to 14.86 by 15% and in air was increased from 12.9 to 15.46 by 20%. Radiation process could improve the wetting performance perhaps by increasing the oxygen functional group concentration, as shown by XPS, and enhancing the polarity of the fiber surface. The increasing of the total surface free energy and the polar component appears to be due to the increasing in the content of surface polar groups for the irradiated fibers. Especially, polar oxygenic groups decrease the contact angle of the fibers by the solution. Therefore, the wettability of the Armos fibers was improved, too.

TABLE V
Surface Roughness of Armos Fibers

Specimen	MVPH (nm)	SR (nm)
Untreated	43.3	52.3
600 kGy + N_2	72.6	84.8
600 kGy + air	52.0	61.6

TABLE VI
Surface Free Energy of Armos Fibers

	Surface energy (mJ/m^2)		
	γ_l^T	γ_l^d	γ_l^p
Untreated	18.58	5.68	12.9
600 kGy + N_2	23.05	8.19	14.86
600 kGy + air	22.92	7.46	15.46

CONCLUSIONS

The effects of γ-ray radiation upon Armos fiber surface have been studied by means of several characterization techniques. The interfacial property (ILSS) of Armos fiber/epoxy resin composites, which employed radiation treated Armos fibers, showed improvement compared with that of the composite, which employed nonsurface-treated Armos fibers. The optimal irradiation dose was 600 kGy and the increasing values of about 17.7 and 15.8% in N_2 and in air medium, respectively. It indicated that the adhesion between Armos fiber and epoxy matrix was effectively improved by γ-ray irradiation. This was ascribed to the increasing of the polar oxygen-containing functional groups and the rough surface obtained by γ-ray irradiation. Thus, γ-ray irradiation further enhanced the wettability of fibers and matrix

and improved the surface free energy. The single fiber intrinsic tensile strength kept steady. That is to say γ-ray irradiation did not essentially damage the mechanical strength of Armos fibers, or the damage degree could be actually ignored. This resulted from the bond strength between the core and skin which was improved through slightly changing the crystallinity of Armos fibers by γ-ray irradiation. The conclusion can be drawn from the experimental results that γ-ray radiation is an effective approach to aramid fiber surface modification.

The authors appreciate the Institute of Chemistry, Chinese Academy of Sciences for their help with XPS measurements.

References

1. Perepelkin, K. E.; Machalaba, N. N.; Budnitski, G. A. Chem Fibers Int 1999, 49, 211.
2. Lin, T. K.; Wu, S. J.; Lai, J. G. Compos Sci Technol 2000, 60, 1873.
3. Park, S. J.; Seo, M. K.; Ma, T. J. J Colloid Interface Sci 2002, 252, 249.
4. Wu, G. M.; Hung, C. H.; You, J. H. J Polym Res 2004, 11, 31.
5. Lin, J. S. Eur Polym J 2002, 38, 79.
6. Yue, C. Y.; Padmanabhan, K. Compos B 1999, 30, 205.
7. Fan, G. N.; Zhao, J. C.; Zhang, Y. K. Polym Bull 2006, 56, 507.
8. Cheng, X. H.; Wu, J. J Appl Polym Sci 2004, 92, 1037.
9. Liu, L; Huang, Y. D.; Zhang, Z. Q. J Appl Polym Sci 2005, 99, 3172.
10. Qiu, Y.; Shao, X.; Jensen, C. Polym Surf 2004, 3, 3.
11. Hwang, Y. J.; Qiu, Y.; Zhang, C. J Adhes Sci Technol 2003, 17, 847.
12. Joung, M. P.; Dae, S. K.; Sung, R. K. J Colloid Interface Sci 2003, 264, 431.
13. Luo, S. J.; Ooij, W. J. J Adhes Sci Technol 2002, 16, 1715.
14. Andrzej, G. C.; Mohammad, H. S.; Shamshad, A. Nucl Instrum Methods Phys Res Sect B 2005, 236, 44.
15. El-Neser, E. M. Polym Adv Technol 2005, 16, 489.
16. Hu, Z. Q.; Zhang, Z. C. Macromol 2006, 39, 1384.
17. Geng, H. W.; Wang, M. Z.; Ge, X. W. Polym Eng Sci 2006, 46, 1748.
18. Flavia, M.; Lúcia, H. I. M.; Silvano, L. Radiat Phys Chem 2004, 71, 255.
19. Alkassiri, H. Radiat Phys Chem 2005, 73, 61.
20. Hua, D. B.; Cheng, K.; Bai, R. Polym Int 2004, 53, 821.
21. Caykara, T.; Yerlikaya, Z.; Kantoglu, O. J Appl Polym Sci 2004, 91, 1893.
22. Zhang, F. Y.; Hou, Z. C.; Sheng, K. L. J Mater Chem 2006, 16, 1215.
23. Watson, G. S.; Busfield, W. K. Polym Int 2005, 54, 1047.
24. Khalil, M. M. I.; El-Sawy, N. M.; El-Shobaky, G. A. J Appl Polym Sci 2006, 102, 506.
25. Bucio, E.; Skewes, P.; Burillo, G. Nucl Instrum Methods Phys Res Sect B 2005, 236, 301.
26. Akhavan, J.; Kronfli, E. Polymer 2003, 44, 7617.
27. Murphy, J. J.; Wetteland, C. J. Nucl Instrum Methods Phys Res Sect B 2005, 236, 223.
28. Chen, J. H.; Asano, M.; Yamaki, T. J Power Sources 2006, 158, 69.
29. Zenkiewicz, M.; Rauchfleisz, M.; Czuprynska, J. Radiat Phys Chem 2003, 68, 799.
30. Hiroki, A.; Asano, M.; Yamaki, T. Chem Phys Lett 2005, 406, 188.
31. Dargaville, T. R.; Elliott, J. M.; Celina, M. J Polym Sci Part B: Polym Phys 2006, 44, 3253.
32. Yamanaka, A.; Izumi, Y.; Kitagawa, T. J Appl Polym Sci 2006, 101, 2619.
33. Yamanaka, A.; Izumi, Y.; Terada, T. J Appl Polym Sci 2006, 100, 5007.
34. Li, J. Q.; Huang, Y. D.; Xu, Z. W. Mater Chem Phys 2005, 94, 315.
35. Zhang, C. H.; Huang, Y. D.; Zhao, Y. D. Mater Chem Phys 2005, 92, 245.
36. Feldman, A. Y.; Gonzalez, M. F.; Wachtel, E. Polymer 2004, 45, 7239.
37. Hsieh, Y. L.; Wu, M.; Andres, D. J Colloid Interface Sci 1991, 144, 127.
38. Wang, Y. Z. Handbook of Chemistry; Beijing University Press: Beijing, 1997.
39. Lange, P. J.; Akker, P. G.; Maas, A. J. H. Surf Interface Anal 2001, 31, 1079.